Least-squares dynamic approximation method for evolution of uncertainty in initial conditions of dynamical systems

Carlos Pantano*
Department of Mechanical Science and Engineering, University of Illinois at Urbana-Champaign, Urbana, Illinois 61801, USA

Babak Shotorban
Center for Simulation of Advanced Rockets, University of Illinois at Urbana-Champaign, Urbana, Illinois 61801, USA

(Received 1 July 2007; revised manuscript received 26 September 2007; published 20 December 2007)

We describe an approximation method to solve the probability density function transport equation, i.e., the Liouville equation, which is encountered in the evolution of uncertainty of the initial values of dynamical systems. A state-space based method is formulated using a least-squares technique that preserves the parabolic nature of the Liouville equation and is flexible in terms of accuracy of representation. This method is based on a global approximation in terms of analytical elementary functions with unknown parameters, whose evolution equations are determined by a global least-squares approximation. The realizability conditions of the probability density, i.e., the non-negativity and normalization conditions are enforced at all times. The method is successfully evaluated in a number of scenarios including the uncertainty evolution in a system governed by a Riccati equation and a particle moving in a fluid under the influence of Stokes drag force. The results obtained in our examples exhibit a reasonable good agreement when compared with the solution of the probability transport equation using the method of characteristics. The cost of the method is proportional to the cost of solving the deterministic system and the number of parameters used to approximate the probability density function, a feature that can make the present method very advantageous in comparison with other methods in problems involving a large number of dimensions.

DOI: 10.1103/PhysRevE.76.066705 PACS number(s): 05.10.−a, 82.20.Wt, 02.50.−r

I. INTRODUCTION

Chaotic solutions of deterministic systems of differential equations can be studied statistically using a classical statistical description based on probability density functions (PDF). In this approach, as opposed to working with stochastic differential equations, a transport PDF equation (TPE) is derived from the governing equations of the system. In the case of evolution of initial or propagation of boundary data uncertainty through a deterministic system, the PDF problem can be stated through the Liouville equation [1–5]. The main objective of this paper is to develop a method to efficiently approximate the solution of the Liouville equation encountered in the evolution of uncertainties in initial conditions.

We consider a system governed by ordinary differential equations, given by

$$\frac{d\boldsymbol{X}}{dt} = \boldsymbol{F}(\boldsymbol{X},t), \tag{1}$$

where $\boldsymbol{X}(t)$ is a vector and $\boldsymbol{F}$ is a vector function. This deterministic system can be solved given the initial value $\boldsymbol{X}(t=0)=\boldsymbol{X}_o$. When uncertainty in the initial value exists, $\boldsymbol{X}_0$ becomes a random vector with known distribution. Sampling independent initial conditions, $\boldsymbol{X}_0$, from this distribution leads to realizations of the trajectories $\boldsymbol{X}(t)$ through Eq. (1). The one-time PDF associated with this system of equations is denoted by $P(\boldsymbol{\xi};t)$, where $\boldsymbol{\xi}=\{\xi_1,\xi_2,\ldots,\xi_N\}$ is the state-space vector of random variables $\boldsymbol{X}=\{X_1,X_2,\ldots,X_N\}$, and semi-colon is used to denote the fact that P depends parametrically on time.

The transport equation for $P(\boldsymbol{\xi};t)$, known as the Liouville equation, can be obtained using continuity of probability in state space, giving

$$\frac{\partial P}{\partial t} + \frac{\partial}{\partial \boldsymbol{\xi}}[\boldsymbol{F}(\boldsymbol{\xi},t)P] = 0. \tag{2}$$

Summation with respect to the individual elements, ξ_i with $i=1\ldots N$, is implied in Eq. (2). Many practical problems of interest lead to large state-space dimensions and insurmountable difficulties arise when trying to solve this high-dimensional equation. In other words, increasing computational cost associated with the additional dimensionality of the PDF (one dimension for each state-space variable) acts as an obstacle in almost all practical cases where there is no analytical solution for this equation. Direct approximation methods, such as the method of characteristics (MC) [2,6,7], finite-difference, finite-volume, finite-element, and spectral methods, directly applied to the space of independent variables $\boldsymbol{\xi}$, in order to carry out the space discretization, lead to tremendously large computational problems that are impractical to solve with current computational resources unless the state-space dimension is very small [8,9]. Therefore, in practice, one needs to consider approximate methods.

The Liouville equation is a special case of the Fokker-Planck equation where the diffusion term is absent [10]. Generally, the approximate methods to solve this equation are limited to the moment methods or Lagrangian particle-based methods. However, the former suffers from large accuracy degradation in situations where the PDF develops a

*Corresponding author: cpantano@uiuc.edu

multimodal structure since a finite number of moments, by themselves, are not generally large enough to recover the shape of the PDF. These PDF's typically describe bistable or metastable states of the system that must be accurately captured in order to make correct predictions. When this occurs, many computational approaches, apart from direct methods, exhibit large accuracy degradation. The particle-based method is the most popular technique used to solve Eq. (2) since it can deal with a large number of state-space variables; however the cost effectiveness of this method is strongly dependent on the nature of the system of equations.

Approximate methods to solve Fokker-Planck type equations include the polynomial chaos (PC) expansion method [11–15], the quadrature method of moments (QMOM) [16,17] and the direct quadrature method of moments (DQMOM) [18–22]. The polynomial chaos family of methods avoid working with the PDF, and instead they operate directly with a spectral representation in terms of random variables. This approach generally leads to algorithms that have a high computational cost in high-dimensional state spaces and its range of applicability is limited to problems with moderate nonlinearities [23]. On the other hand, DQMOM, where the PDF is approximated as a sum of Dirac's delta functions with evolving parameters, has a number of desirable advantages. This includes a finite and predetermined cost which is given by the presumed function form and exhibit reasonable capability to adaptation. However, the use of generalized functions (Dirac's delta function) mandates the use of moment methods and this inevitably introduces the limitations of the Hausdorff moment problem [24], which affect the ability to reconstruct the PDF from its known moments. Other approaches not using the delta function rely on a linear combination of smooth partial PDFs [25], where the governing equations for the weights and partial PDFs are derived by a separation-of-variables technique. Most of these global approximation techniques can be consider as Rayleigh-Ritz methods which differ by the choice of global approximation function and the type of minimization statement being used to derive the equations [26]. These methods are widely used in the analysis of vibrations in structures as well as in quantum chemistry to solve differential equations when the true solutions are intractable or exceedingly complex.

According to the definition of the PDF, any approximation method must satisfy at least two realizability conditions, which are the non-negativity property,

$$P(\boldsymbol{\xi};t) \geqslant 0, \tag{3}$$

and the normalization condition

$$\int_{-\infty}^{\infty} P(\boldsymbol{\xi};t)d\xi = 1, \tag{4}$$

at every instant in time. For the PDF model to be a realistic probability measure, all moments must also exist. From a modeling point of view, an approximation fidelity improves and its cost decreases if some knowledge about the behavior and dependence of a solution is available. This can be prior knowledge, or information obtained by solving the problem with increasingly accurate approximations (the usual practice). This observation can be exploited in two ways when dealing with PDFs. First, the general shapes of many PDFs encountered in practice have been measured experimentally to a good degree of accuracy and furthermore, it has been observed that the state space of the random variables is not fully sampled by the PDF [27]. This observation can be used advantageously when designing state-space based approximations. In many cases, very accurate techniques are only required when the interest is focused on the precise behavior of the tails of the PDF or, equivalently, the high-order moments of the random variables. When this is the case, the computational solution can be very expensive if no prior knowledge of the shape of the PDF is available. In many other cases, only a reasonably good (practical) approximation is desired. This implies accurate mode(s) location(s), width and magnitude since this corresponds to the regions in state space that have the largest probability density.

In the current work, we propose a new approximation method that involves a combination of the elements used in DQMOM and the partial PDF approach [25]. The current proposition is a global approximation method based on a least-squares minimization. Similar techniques are used in different fields to approximate functions of different natures [28–34]. The present approach consists in modeling PDFs as a sum of smooth functions, with unknown parameters that are functions of time. In fact, similar PDF representations are well known in the statistical community, although not applied to dynamical systems. The notion of decomposing the PDF into elements is not new [35] and it has been used to approximate experimentally measured data in geophysical problems [36]. A good number of properties and limitations of this technique are known, but roughly speaking, the limitations imposed by the Hausdorff theorem, that applies to all moment based techniques, can be avoided. The elemental shape functions used in this method are called kernel density functions (KDF) [37–39]. It is emphasized that the equations for the unknown parameters resulting from our approximation technique are not of the same nature as those from DQMOM or [25], but they are the result of a minimization problem in state space. We should mention that a constrained-minimization technique to derive the weights of the KDF that best approximate an experimentally measured PDF given by its moments has been used in the past [39]. This approach differs from the approach proposed in our current study in which the minimization is dynamic and based on a governing differential equation.

II. PROBLEM STATEMENT

As will become apparent in some of the examples to be presented, it is convenient to consider a generalization of Eq. (2) in which the state-space variables are partitioned into $\boldsymbol{\xi} = \boldsymbol{\xi}_L \cup \boldsymbol{\xi}_G$ with $\boldsymbol{\xi}_L = \{\xi_1, \xi_2, \ldots, \xi_{N_L}\}$ and $\boldsymbol{\xi}_G = \{\xi_{N_L+1}, \xi_{N_L+2}, \ldots, \xi_N\}$, where $N_L < N$. The state-space variable $\boldsymbol{\xi}_L$ will be treated in a classical way, while $\boldsymbol{\xi}_G$ will be treated with the global representation proposed here. Practically, we should choose N_L as small as possible to avoid the large dimensionality cost of PDF transport equations while

taking $N_G=N-N_L$ as large as possible. Eq. (2) is now written in the form

$$\frac{\partial P}{\partial t}+\frac{\partial}{\partial \boldsymbol{\xi}_L}[\boldsymbol{F}_L(\boldsymbol{\xi},t)P]+\mathcal{Q}(\boldsymbol{\xi},t,P)=0, \tag{5}$$

where $P(\boldsymbol{\xi};t)=P(\boldsymbol{\xi}_G;\boldsymbol{\xi}_L,t)$ denotes a function of $\boldsymbol{\xi}_G$, $\boldsymbol{\xi}_L$, and t. This notation is introduced for convenience to clarify the developments that follow. The quantity $\boldsymbol{F}_L$ denotes that part of $\boldsymbol{F}$ corresponding to $\boldsymbol{\xi}_L$ and $\mathcal{Q}$ is the remaining terms; generally a linear functional on P that depends explicitly on $\boldsymbol{\xi}$. In some settings, $\mathcal{Q}$ can involve state-space derivatives, as in Eq. (2), and/or integrals.

We now seek a global approximation of an arbitrary PDF of the form

$$P(\boldsymbol{\xi};t)=\alpha_m(\boldsymbol{\xi}_L,t)P_m[\boldsymbol{\xi}_G,\boldsymbol{\mu}^m(\boldsymbol{\xi}_L,t)], \tag{6}$$

where $m=1,\ldots,M$ and repeated subscripts imply summation, unless stated otherwise. Each P_m is a non-negative function that depends parametrically on $\boldsymbol{\mu}^m(\boldsymbol{\xi}_L,t)=\{\mu_1^m(\boldsymbol{\xi}_L,t),\mu_2^m(\boldsymbol{\xi}_L,t),\ldots,\mu_{L_m}^m(\boldsymbol{\xi}_L,t)\}$. L_m is the dimension of the vector $\boldsymbol{\mu}^m$ with components $\mu_j^m(\boldsymbol{\xi}_L,t)$. Our function choice for P_m is such that by construction

$$\int_{-\infty}^{\infty}P_m(\boldsymbol{\xi}_G,\boldsymbol{\mu}^m)d\boldsymbol{\xi}_G=1, \quad \forall\, m, \tag{7}$$

with moments given by

$$\boldsymbol{\eta}^{z,m}(\boldsymbol{\xi}_L,t)=\int_{-\infty}^{\infty}\boldsymbol{\xi}^z P_m(\boldsymbol{\xi}_G,\boldsymbol{\mu}^m)d\boldsymbol{\xi}_G. \tag{8}$$

The normalization condition requires

$$1=\int_{-\infty}^{\infty}\alpha(\boldsymbol{\xi}_L,t)d\boldsymbol{\xi}_L, \tag{9}$$

where

$$\alpha(\boldsymbol{\xi}_L,t)=\sum_{m=1}^{M}\alpha_m(\boldsymbol{\xi}_L,t), \tag{10}$$

that along with non-negativity condition of P_m implies $\alpha_m \geqslant 0$. It is emphasized that Eq. (6) should not be seen as a separation-of-variables approximation but as a global approximation of the Rayleigh-Ritz type. The functions P_m are specified beforehand and are essentially elementary presumed PDF functions, or KDF as referred to in the statistical literature [37]. In general, Eq. (6) does not satisfy Eq. (2) exactly and a projection technique must be used to determine the unknown dependent quantities. If necessary, the moments of the PDF are determined through the familiar formulas, giving in our case

$$\langle \xi_l^z\rangle=\begin{cases}\displaystyle\int_{-\infty}^{\infty}\xi_l^z\alpha(\boldsymbol{\xi}_L,t)d\boldsymbol{\xi}_L, & \text{for } l=1,\ldots,N_L,\\ \displaystyle\int_{-\infty}^{\infty}\eta_l^{z,m}(\boldsymbol{\xi}_L,t)\alpha_m(\boldsymbol{\xi}_L,t)d\boldsymbol{\xi}_L, & l=N_L+1,\ldots,N,\end{cases} \tag{11}$$

where angle brackets denote expectations (averages).

We propose to determine the governing equations for α_m and μ_j^m in Eq. (6) by a least-squares technique in the $\boldsymbol{\xi}_G$ domain. We seek the closest approximation to the PDF that can be obtained at each instant with a function of the form shown in Eq. (6). To this end, we define the residual of Eq. (2) as

$$r(\boldsymbol{\xi};t)=P_m\frac{\partial\alpha_m}{\partial t}+\alpha_m\left[\frac{\partial P_m}{\partial\mu_j^m}\frac{\partial\mu_j^m}{\partial t}+\mathcal{Q}(\boldsymbol{\xi},t,P_m)\right]+\frac{\partial}{\partial\boldsymbol{\xi}_L}[\boldsymbol{F}_L(\boldsymbol{\xi},t)\alpha_m P_m]. \tag{12}$$

Introducing the short-hand notation

$$\frac{\partial\alpha_m}{\partial t}=\dot{\alpha}_m, \quad \frac{\partial\mu_j^m}{\partial t}=\dot{\mu}_j^m, \tag{13}$$

and

$$\mathbf{1}=\{1,1,\ldots,1\}^T, \tag{14}$$

$$\boldsymbol{\alpha}=\{\alpha_1,\alpha_2,\ldots,\alpha_M\}^T, \tag{15}$$

$$\boldsymbol{\mu}=\{\mu_1^1,\mu_2^1,\ldots,\mu_{L_1}^1,\mu_1^2,\mu_2^2,\ldots,\mu_{L_2}^2,\ldots,\mu_1^M,\mu_2^M,\ldots,\mu_{L_M}^M\}^T, \tag{16}$$

$$\boldsymbol{P}=\{P_1,P_2,\ldots,P_M\}^T, \tag{17}$$

$$\mathcal{M}=\frac{\partial\boldsymbol{P}}{\partial\boldsymbol{\mu}}=\begin{pmatrix}\frac{\partial P_1}{\partial\mu_1^1} & \frac{\partial P_1}{\partial\mu_2^1} & \ldots & \frac{\partial P_1}{\partial\mu_{L_1}^1} & 0 & 0 & \ldots & 0 & \ldots\\ 0 & 0 & \ldots & 0 & \frac{\partial P_2}{\partial\mu_1^2} & \frac{\partial P_2}{\partial\mu_2^2} & \ldots & \frac{\partial P_2}{\partial\mu_{L_2}^2} & \ldots\\ 0 & 0 & \ldots & 0 & 0 & 0 & \ldots & 0 & \ldots\end{pmatrix}, \tag{18}$$

$$\boldsymbol{Q}=\{\mathcal{Q}(\boldsymbol{\xi},t,P_m)\}^T, \tag{19}$$

we obtain

$$r(\boldsymbol{\xi},\boldsymbol{\alpha},\boldsymbol{\mu},\dot{\boldsymbol{\alpha}},\dot{\boldsymbol{\mu}})=\boldsymbol{P}^T\dot{\boldsymbol{\alpha}}+\boldsymbol{\alpha}^T\mathcal{M}\dot{\boldsymbol{\mu}}+\boldsymbol{\alpha}^T\boldsymbol{Q}+(\boldsymbol{F}_L\boldsymbol{\alpha}^T\boldsymbol{P})_{\boldsymbol{\xi}_L}. \tag{20}$$

An approximation of Eq. (5) can be constructed by making $\|r\|$ as small as possible, where $\|.\|$ is a suitable norm. The choice of the norm under which r reaches a minimum generally determines the type of approximation. In our case, we

choose to minimize the integral of the square residual in $\boldsymbol{\xi}_G$ space, an approximation which is also known as a least-squares method. Moreover, we incorporate the normalization condition, Eq. (9), using a Lagrange multiplier approach [40]. The final cost function, at each $\boldsymbol{\xi}_L$ location, is given by

$$\delta J(\boldsymbol{\xi}_L, \boldsymbol{\alpha}, \boldsymbol{\mu}, \dot{\boldsymbol{\alpha}}, \dot{\boldsymbol{\mu}}, \lambda) = \int_{-\infty}^{\infty} r^2 d\boldsymbol{\xi}_G + \lambda(t)\mathbf{1}^T\dot{\boldsymbol{\alpha}}, \tag{21}$$

where $\lambda(t)$ is a Lagrange multiplier that enforces the constraint, through the time rate of change of Eq. (9), such that the total cost function is given by

$$J(t,\lambda) = \int_{-\infty}^{\infty} \delta J(\boldsymbol{\xi}_L, \boldsymbol{\alpha}, \boldsymbol{\mu}, \dot{\boldsymbol{\alpha}}, \dot{\boldsymbol{\mu}}, \lambda) d\boldsymbol{\xi}_L. \tag{22}$$

The costs functions J coincides with δJ for $N_L=0$. The evolution equations for $\boldsymbol{\alpha}$ and $\boldsymbol{\mu}$ are derived by developing these integrals and performing the minimization. We introduce the scalar, vector and matrix functions

$$\mathcal{A} = \int_{-\infty}^{\infty} \boldsymbol{P}\boldsymbol{P}^T d\boldsymbol{\xi}_G, \tag{23}$$

$$\mathcal{B} = \int_{-\infty}^{\infty} \mathcal{M}^T \boldsymbol{\alpha}\boldsymbol{\alpha}^T \mathcal{M}\, d\boldsymbol{\xi}_G, \tag{24}$$

$$\mathcal{C} = 2\int_{-\infty}^{\infty} \mathcal{M}^T \boldsymbol{\alpha}\boldsymbol{P}^T d\boldsymbol{\xi}_G, \tag{25}$$

$$\boldsymbol{D} = 2\int_{-\infty}^{\infty} \{\boldsymbol{\alpha}^T\boldsymbol{Q} + (\boldsymbol{F}_L\boldsymbol{\alpha}^T\boldsymbol{P})_{\boldsymbol{\xi}_L}\}\boldsymbol{P}\, d\boldsymbol{\xi}_G, \tag{26}$$

$$\boldsymbol{E} = 2\int_{-\infty}^{\infty} \{\boldsymbol{\alpha}^T\boldsymbol{Q} + (\boldsymbol{F}_L\boldsymbol{\alpha}^T\boldsymbol{P})_{\boldsymbol{\xi}_L}\}\mathcal{M}^T\boldsymbol{\alpha}\, d\boldsymbol{\xi}_G, \tag{27}$$

$$f = \int_{-\infty}^{\infty} \{\boldsymbol{\alpha}^T\boldsymbol{Q} + (\boldsymbol{F}_L\boldsymbol{\alpha}^T\boldsymbol{P})_{\boldsymbol{\xi}_L}\}^2 d\boldsymbol{\xi}_G, \tag{28}$$

and express Eq. (21) according to

$$\delta J = \dot{\boldsymbol{\alpha}}^T\mathcal{A}\dot{\boldsymbol{\alpha}} + \dot{\boldsymbol{\mu}}^T\mathcal{B}\dot{\boldsymbol{\mu}} + \dot{\boldsymbol{\mu}}^T\mathcal{C}\dot{\boldsymbol{\alpha}} + \boldsymbol{D}^T\dot{\boldsymbol{\alpha}} + \boldsymbol{E}^T\dot{\boldsymbol{\mu}} + f + \lambda\mathbf{1}^T\dot{\boldsymbol{\alpha}}. \tag{29}$$

In the case where $N_L>0$, the system must be discretized in $\boldsymbol{\xi}_L$ space and Eq. (21) must be written in terms of the discretized variables. The resulting equations are exactly of the same form except that the integral of the Lagrange multiplier appearing in the right-hand side of Eq. (22) is transformed into a sum.

The system of equations governing the evolution of $\boldsymbol{\alpha}$ and $\boldsymbol{\mu}$ can be derived by minimizing the quadratic form, Eq. (29), with respect to $\dot{\boldsymbol{\alpha}}$ and $\dot{\boldsymbol{\mu}}$. The resulting system of equations, preserving the parabolic nature of the Liouville equation in time, is quasilinear with nonlinear coefficients. This system is given by

$$\begin{pmatrix} 2\mathcal{A} & \mathcal{C}^T \\ \mathcal{C} & 2\mathcal{B} \end{pmatrix}\begin{pmatrix} \dot{\boldsymbol{\alpha}} \\ \dot{\boldsymbol{\mu}} \end{pmatrix} = -\begin{pmatrix} \boldsymbol{D} + \lambda I \\ \boldsymbol{E} \end{pmatrix}. \tag{30}$$

The coefficients resulting from the state-space integration that appears in the elements of $\mathcal{A}$, $\mathcal{B}$, $\mathcal{C}$, $\boldsymbol{D}$, and $\boldsymbol{E}$ can be determined beforehand; currently we use symbolic manipulation software to obtain their algebraic expressions. We observe that f does not need to be computed. This is fortunate since it is often the most difficult (nonlinear) quadrature to calculate. In the rest of the manuscript, we will refer to the newly introduced method as the least-squares kernel-density (LSQKD) method.

III. UNIDIMENSIONAL STATE-SPACE EXAMPLE

As an example of the LSQKD technique previously discussed, we consider a problem first solved analytically by Ehrendorfer [2], which is the Liouville equation corresponding to the Riccati ordinary differential equation

$$\dot{X} = aX^2 + bX + c, \tag{31}$$

with $X(0)=X_o$ specified. This initial condition is known through its PDF, $P(X_o;0)$, whose evolution is governed by the Liouville equation

$$\frac{\partial P}{\partial t} + \frac{\partial}{\partial \xi}((a\xi^2 + b\xi + c)P) = 0. \tag{32}$$

This equation can be solved by the method of characteristics [2], giving

$$P(\xi;t) = \frac{P(\Xi,0)}{\gamma^2}\exp\left(bt + \frac{2r_1}{\gamma}\ln[\Xi a(e^{-\gamma t}-1) - r_2 + r_1 e^{-\gamma t}] - \frac{2r_2}{\gamma}\ln[\Xi a(1-e^{\gamma t}) + r_1 - r_2 e^{\gamma t}]\right), \tag{33}$$

where

$$\Xi(\xi,t) = \frac{1}{a}\left[\frac{a\xi(r_2 e^{\gamma t} - r_1) + r_1 r_2(e^{\gamma t}-1)}{a\xi(1-e^{\gamma t}) - r_1 e^{\gamma t} + r_2}\right], \tag{34}$$

and the constants

$$r_1 = \frac{b}{2} + \Delta^{1/2}, \quad r_2 = \frac{b}{2} - \Delta^{1/2}, \quad \gamma = r_1 - r_2, \quad \Delta = \frac{b^2}{4} - ac > 0. \tag{35}$$

The LSQKD method is now applied to the evolution of the PDF, Eq. (32), modeled by a single KDF with a Gaussian shape of the form

$$P(\xi;t) = G(\xi,\mu,\sigma) \equiv \frac{1}{\sqrt{2\pi}\sigma}\exp\left[-\frac{(\xi-\mu)^2}{2\sigma^2}\right], \tag{36}$$

where μ and σ are the mean and standard deviation, respectively, which are functions of time. Since the initial condition has a Gaussian shape [2], it is reasonable to choose this function as the approximation. It is noted that there are no theoretical limitations on the form of the approximating function, as long as the realizability constraints, i.e., Eqs. (3)

and (4), are satisfied. Corresponding to the formulation given in Sec. II, the constants $M=1$, $L_1=2$ and the weighting $\alpha_1=1$ is predetermined since only one presumed function is used. With the parameters $\boldsymbol{\mu}=\{\mu,\sigma\}$ and $\boldsymbol{\xi}_G=\{\xi\}$, the system of differential equations (30) is constructed and solved numerically.

After some algebraic manipulations and observing that we only need to consider the terms involving $\boldsymbol{\mu}_t=\dot{\boldsymbol{\mu}}$ since α_1 is constant, we obtain

$$\boldsymbol{\mathcal{B}}=\begin{pmatrix} \dfrac{1}{4\sqrt{\pi}\sigma^3} & 0 \\ 0 & \dfrac{3}{8\sqrt{\pi}\sigma^3} \end{pmatrix}, \tag{37}$$

$$\boldsymbol{E}=\begin{pmatrix} -\dfrac{2c+2(b+a\mu)\mu-a\sigma^2}{4\sqrt{\pi}\sigma^3} & -\dfrac{3(2a\mu+b)}{4\sqrt{\pi}\sigma^2} \end{pmatrix}, \tag{38}$$

where $\boldsymbol{\mathcal{B}}$ and $\boldsymbol{E}$ are given by Eq. (24) and Eq. (27), respectively. These quantities are then used to minimize the functional

$$J=\dot{\boldsymbol{\mu}}^T\boldsymbol{\mathcal{B}}(\boldsymbol{\mu})\dot{\boldsymbol{\mu}}+\boldsymbol{E}^T(\boldsymbol{\mu})\dot{\boldsymbol{\mu}}+f, \tag{39}$$

that leads to the system of quasilinear differential equations

$$\dot{\boldsymbol{\mu}}=-\frac{1}{2}\boldsymbol{\mathcal{B}}^{-1}(\boldsymbol{\mu})\boldsymbol{E}(\boldsymbol{\mu})=\begin{pmatrix} c+b\mu+a\mu^2-\dfrac{a\sigma^2}{2} \\ (b+2a\mu)\sigma \end{pmatrix}. \tag{40}$$

We present results for the two cases discussed in [2], both corresponding to the parameters $a=-1$, $b=1$, and $c=2$ used in that reference. The initial condition is Gaussian with $\sigma(0)=\sqrt{0.1}$ and mean distribution $\mu(0)=-2$ and $\mu(0)=0$ in the first and second cases, respectively. The calculations are carried out to $t=T$, where $T=0.3$ and 0.6 in the first and second cases, respectively. These parameters are identical to those used in [2].

Figures 1(a) and 1(b) compare the exact results given in Eq. (33) with the LSQKD method at times $T/2$ and T during the evolution. As can be seen, the predictions of the present method are quite reasonable, given that it has to fit the PDF form to a single Gaussian shape. Deviation between exact and approximate results increase, and are more pronounced as time grows. This deviation is more notable in the tails of the PDF.

In practice, approximate PDF methods focus on accurately capturing the mode(s) of the PDF. In some cases, where bifurcation occurs, it is desirable to be able to reproduce the dynamics of multimodal behavior, a topic that we are currently exploring. Additionally, it is important to point out that the cost of the approximation method we develop here is small. This cost is comparable to that of solving the ordinary differential equation Eq. (31), approximately twice as that of solving Eq. (31). This is possible only because all the quadratures, Eq. (21), can be analytically performed beforehand, in our case using symbolic manipulation software.

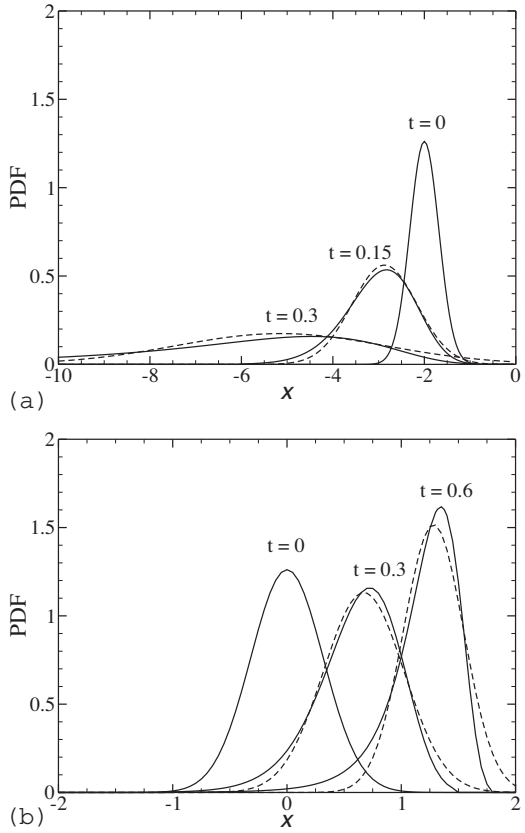

FIG. 1. PDF evolution at different times for the following cases: (a) Unstable behavior (evolution from right to left) and (b) stable behavior (evolution from left to right). Continuous line denotes exact solution and broken line denotes LSQKD.

IV. MULTIDIMENSIONAL STATE-SPACE EXAMPLE

As a benchmark multidimensional case, the LSQKD method is applied to the evolution of uncertain initial position, velocity and temperature of a particle released in a one-dimensional fluid flow. This is a one-dimensional model of more realistic two- and three-dimensional cases which are of practical interest. Although it may appear that this problem is too simplistic, the base flow spatial dependence can introduce such a strong nonlinearity that most approximate methods fail to predict the behavior of the PDF [23].

Let x_p, u_p, and T_p describe the particle instantaneous position, velocity and temperature, respectively, governed by

$$\frac{dx_p}{dt}=u_p, \tag{41}$$

$$\frac{du_p}{dt}=\frac{1}{\tau_p}[\phi(x_p,t)-u_p], \tag{42}$$

$$\frac{dT_p}{dt}=\frac{1}{\tau_T}[\theta(x_p,t)-T_p], \tag{43}$$

where $\tau_p=\rho_p d_p^2/18\nu$ and $\tau_T=C_p\rho_p d^2/12k_f$ are the particle relaxation time and the thermal relaxation time, respectively. The parameters ρ_p and d_p representing the density and diameter of the particle, respectively, ν denotes the viscosity of

the surrounding fluid phase, C_p is the specific heat of the particle, and k_f is the effective conductivity of the fluid. In Eq. (42), ϕ is the velocity field of the fluid phase and $\phi(x_p,t)$ denotes the fluid-phase velocity at the location of the particle. Similarly, θ denotes the temperature field of the fluid phase and $\theta(x_p,t)$ denotes the fluid-phase temperature at the location of the particle. In this formulation, it is assumed that the force acting on the particle can be approximated by the Stokes drag only. We also assume that the thermal inertia of the fluid is large, such that only the particles change their temperature depending on whether the fluid has a higher or lower temperature than the particle. The fluid does not change its thermodynamic state in this approximation. Given the fluid-phase velocity $\phi(x,t)$ and temperature $\theta(x,t)$, and initial particle position $x_p(0)$, velocity $u_p(0)$, and temperature $T_p(0)$, the set of Eqs. (41)–(43) can be solved for $x_p(t)$, $u_p(t)$, and $T_p(t)$.

Suppose that uncertainties in the initial values of particle position, velocity, and temperature can be represented by one-time joint PDF, $P(x,u,T;t=0)$, where x, u, and T represent the state-space variables corresponding to x_p, u_p, and T_p, respectively. Then, $P(x,u,T;t)$ obeys the Liouville equation

$$\frac{\partial P}{\partial t}+\frac{\partial}{\partial x}(uP)+\frac{1}{\tau_p}\frac{\partial}{\partial u}[(\phi(x,t)-u)P]+\frac{1}{\tau_T}\frac{\partial}{\partial T}[(\theta(x,t)-T)P]=0. \tag{44}$$

Since T appears explicitly only in divergence form, it is possible to integrate this equation with respect to T to derive the transport equation for the marginal $P(x,u;t)$, given by

$$\frac{\partial P}{\partial t}+\frac{\partial}{\partial x}(uP)+\frac{1}{\tau_p}\frac{\partial}{\partial u}[(\phi(x,t)-u)P]=0. \tag{45}$$

For simplicity, we chose not to denote the PDF appearing in Eq. (44) and Eq. (45) with different symbols to improve the fluidity of the text and refer to the solution of Eq. (44) as the three-dimensional (3D) state-space problem and to the solution of Eq. (45) as the two-dimensional (2D) state-space problem.

A. Bidimensional state space case

We consider first the problem of the marginal $P(x,u,t)$ obeying Eq. (45) and specialize the fluid-phase velocity to

$$\phi(x,t)=1+\beta\sin(2\pi x). \tag{46}$$

This sinusoidal nonlinearity of ϕ is strong since it cannot be approximated accurately by a finite-degree polynomial over the whole range of x. The particle time constant τ_p is taken equal to unit in Eq. (45). This is equivalent to rescaling time according to t/τ_p and it does not remove generality from the present application. With these values for ϕ and τ_p, the system of differential equations (41) and (42) can be solved numerically for $x_p(t)$ and $u_p(t)$. Equation (45) can be solved by the method of characteristics [2] with a specified initial PDF. Throughout this section, we use the results obtained by the MC to verify the results predicted by the LSQKD method. However, for the special case of $\beta=0$, there is an analytical solution of Eqs. (41) and (42) that we use for the verification of the LSQKD method in this special case.

1. Least-squares global approximation in x-u state space

We choose to approximate $P(x,u;t)$ by a bivariate Gaussian of the form

$$P(x,u;t)=G(\boldsymbol{y},\Lambda)\equiv\frac{\exp\left[-\frac{1}{2}\boldsymbol{y}^T\Lambda^{-1}\boldsymbol{y}\right]}{2\pi[\det(\Lambda)]^{1/2}}, \tag{47}$$

where

$$\boldsymbol{y}=\{x-\mu_x(t),u-\mu_u(t)\}, \tag{48}$$

and Λ is the time-dependent covariance matrix

$$\Lambda=\begin{pmatrix}\sigma_x^2(t) & \sigma_x(t)\sigma_u(t)\rho(t)\\ \sigma_x(t)\sigma_u(t)\rho(t) & \sigma_u^2(t)\end{pmatrix}, \tag{49}$$

with $-1\leqslant\rho(t)\leqslant 1$. The constants $M=1$, $L_1=5$, and the parameter vectors are $\alpha_1=1$ and $\boldsymbol{\mu}=\{\mu_x,\sigma_x,\mu_u,\sigma_u,\rho\}$. According to the formulation given in Sec. II, we have chosen $\boldsymbol{\xi}=\boldsymbol{\xi}_G=\{x,u\}$; both state-space variables are treated globally in this case.

For the special case of $\beta=0$, the system of equations (41) and (42) can be solved analytically when $\phi(x)=1$, giving

$$x_p(t)=[1-u_p(0)][\exp(-t)-1]+t+x_p(0), \tag{50}$$

$$u_p(t)=[u_p(0)-1]\exp(-t)+1, \tag{51}$$

where $x_p(0)$ and $u_p(0)$ are the initial position and velocity of the particle, respectively. Since, Eqs. (50) and (51) are linear in $x_p(0)$ and $u_p(0)$, an exact expression can be developed for the mean particle position $\langle x_p\rangle$ and mean particle velocity $\langle u_p\rangle$ by ensemble averaging of these expressions, giving

$$\langle x_p\rangle(t)=[1-\langle u_p\rangle(0)][\exp(-t)-1]+t+\langle x_p\rangle(0), \tag{52}$$

$$\langle u_p\rangle(t)=(\langle u_p\rangle(0)-1)\exp(-t)+1, \tag{53}$$

where $\langle x_p\rangle(0)$ and $\langle u_p\rangle(0)$ denote the initial mean position and velocity of the one-dimensional particle, respectively. The second order central moments are given by

$$\langle x_p'^2\rangle(t)=\langle u_p'^2\rangle(0)[\exp(-t)-1]^2-2\langle x_p'u_p'\rangle(0)[\exp(-t)-1]+\langle x_p'^2\rangle(0), \tag{54}$$

$$\langle u_p'^2\rangle(t)=\langle u_p'^2\rangle(0)\exp(-2t), \tag{55}$$

$$\langle x_p'u_p'\rangle=\langle u_p'^2\rangle(0)[\exp(-2t)-\exp(-t)]+\langle x_p'u_p'\rangle(0)\exp(-t), \tag{56}$$

where $\langle x_p'^2\rangle=\langle(x_p-\langle x_p\rangle)^2\rangle$, $\langle u_p'^2\rangle=\langle(u_p-\langle u_p\rangle)^2\rangle$, and $\langle x_p'u_p'\rangle=\langle(x_p-\langle x_p\rangle)(u_p-\langle u_p\rangle)\rangle$. These analytical solutions are compared against the results obtained by the LSQKD method using the bivariate Gaussian PDF with initial condition $\mu_x(0)=1$, $\mu_u(0)=2$, $\sigma_x(0)=1$, $\sigma_u(0)=\sqrt{0.2}$, and $\rho(0)=0.5$, which are defined in Eqs. (47)–(49). Figure 2(a) shows the

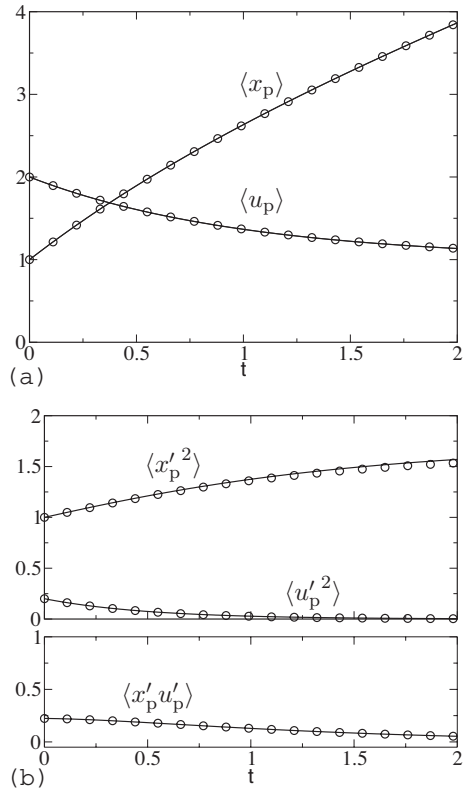

FIG. 2. Time evolution of (a) mean and (b) variances of the particle position and velocity for $\beta=0$ using exact (symbols) and LSQKD (solid lines).

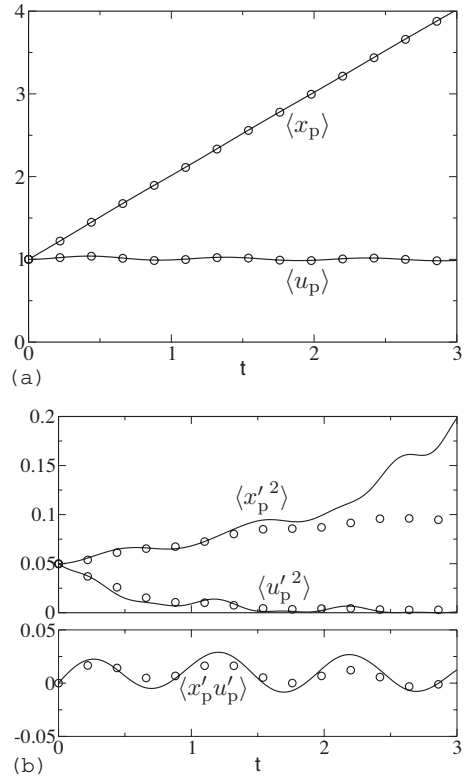

FIG. 3. Evolution of (a) mean and (b) variances of particle position and velocity for $\beta=0.5$ using MC (symbols) and LSQKD (solid lines).

time evolution of the mean position and velocity of the particle obtained through the exact solution and the proposed approximation. Figure 2(b) shows comparisons of the time evolution of the elements of the covariance matrix as well. As can be seen, the agreement is good in this case. We caution that this is not completely surprising since the uncertainty in the initial conditions affects the solution linearly.

For the more general case there is no exact analytical solution for the system of equations (41) and (42) where $\phi(x)=1+\beta\sin(2\pi x)$ with $\beta\neq 0$. Therefore we compare the results obtained by the model proposed in this work to those obtained by the classical method of characteristics (MC) [2,6]. At regular intervals in time, the mean and covariance matrix of the positions and velocities of particles are calculated. Figure 3 shows the time evolution of the mean and variance of the particle position and velocity obtained by LSQKD method and exact solution obtained by MC. In the case shown in this figure $\beta=0.5$, $\mu_x(0)=\mu_u(0)=1$, $\sigma_x(0)=\sigma_u(0)=\sqrt{0.05}$, and $\rho(0)=0$. We observe that the method is able to reproduce the behavior of the means quite accurately but obvious deficiencies are observed for the position variance after some short time. As we will show shortly, these results are not a consequence of a shortcoming in the methodology we present, but rather, a failure of our function choice for the PDF.

2. Least-squares approximation in u space only

The previous example shows that the LSQKD approximation can fail when the function ansatz is unable to accommodate the features of the PDF, induced by the strong nonlinearity of $\phi(x)$. The nonlinearity makes the popular method based on polynomial chaos expansions, impractical for uncertainty quantification in this case. We now proceed to describe the more appropriate function choice for such a nonlinear case using the LSQKD method where only the velocity state-space coordinate is treated globally and position is dealt with locally.

The PDF is now approximated by a function of the form

$$P(x,u;t)=\alpha(x,t)G[u,\mu(x,t),\sigma(x,t)]. \tag{57}$$

Corresponding to the notation introduced is Sec. II, $N_L=1$, $\boldsymbol{\xi}_L=\{x\}$, $\boldsymbol{\xi}_G=\{u\}$, with $F_L=u$,

$$\boldsymbol{\mu}=\{\mu(x,t),\sigma(x,t)\}^T, \tag{58}$$

$$\mathcal{M}=\left(\frac{\partial G}{\partial \mu},\frac{\partial G}{\partial \sigma}\right), \tag{59}$$

and

$$\boldsymbol{Q}(G)=\frac{\partial}{\partial u}\left(\frac{\phi(x)-u}{\tau_p}G\right). \tag{60}$$

After simplifying the least-squares equations it is possible to directly solve for the Lagrange multiplier, $\lambda(t)=0$ in this case, and obtain

$$\frac{\partial \alpha}{\partial t}+\frac{\partial(\mu\alpha)}{\partial x}=0, \tag{61}$$

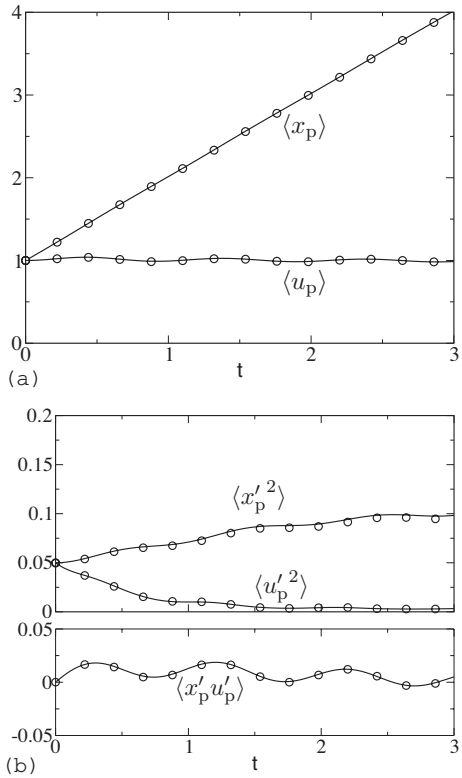

FIG. 4. Evolution of (a) mean and (b) variances of particle position and velocity for $\beta=0.5$ using MC (symbols) and LSQKD (solid lines).

$$\frac{\partial \mu}{\partial t} + \sigma \frac{\partial \ln \alpha}{\partial x} + \frac{\sigma}{2}\frac{\partial \sigma}{\partial x} + \mu \frac{\partial \mu}{\partial x} = \frac{\phi(x) - \mu}{\tau_p}, \tag{62}$$

$$\frac{\partial \sigma}{\partial t} + \frac{\partial (\mu \sigma)}{\partial x} = -\frac{\sigma}{\tau_p}. \tag{63}$$

Furthermore, the statistical moments are calculated according to

$$\langle x_p \rangle(t) = \int_{-\infty}^{\infty} x \alpha(x,t) dx, \tag{64}$$

$$\langle u_p \rangle(t) = \int_{-\infty}^{\infty} \mu(x,t) \alpha(x,t) dx, \tag{65}$$

$$\langle x_p'^2 \rangle(t) = \int_{-\infty}^{\infty} x^2 \alpha(x,t) dx - \langle x_p \rangle(t)^2, \tag{66}$$

$$\langle u_p'^2 \rangle(t) = \int_{-\infty}^{\infty} [\sigma^2(x,t) + \mu^2(x,t)] \alpha(x,t) dx - \langle u_p \rangle(t)^2, \tag{67}$$

and

$$\langle x_p' u_p' \rangle(t) = \int_{-\infty}^{\infty} x \mu(x,t) \alpha(x,t) dx - \langle x_p \rangle(t) \langle u_p \rangle(t). \tag{68}$$

Figure 4 shows the time evolution of the moments with identical initial conditions as those used in the previous subsection for the case with $\beta=0.5$. Equations (61)–(63) are solved by the MC for first-order quasilinear systems of hyperbolic equations [41]. As seen in Fig. 4(b) there is now an improved agreement between the two methods.

Figure 5 presents isocontours of $P(x,u;t)$ at three different times. The initial condition, $t=0$, corresponds to a bivariate Gaussian distribution, which is not shown in this figure. The shape of the PDF deviates strongly from Gaussian as time progresses and eventually evolves into an M shape at $t=3$. It is observed that the new method is able to capture this feature and shows reasonably good agreement with the MC solution.

Further comparisons of the statistics can be derived using the conditional PDFs, defined by

$$P_{x|u}(x|u;t) = \frac{P(x,u;t)}{P_u(u;t)} \tag{69}$$

and

$$P_{u|x}(u|x;t) = \frac{P(x,u;t)}{P_x(x;t)}, \tag{70}$$

where $P_{x|u}$ and $P_{u|x}$ denote conditional PDFs and $P_u(u;t) = \int_{-\infty}^{\infty} P(x,u;t) dx$ and $P_x(x;t) = \int_{-\infty}^{\infty} P(x,u;t) du$ are the marginal PDFs. The marginal $P(x;t) = \alpha(x)$ in the LSQKD method represents the number density of particles in the Eulerian description of particle systems. It is noted that $P_{u|x} = G[u, \mu(x,t), \sigma(x,t)]$ is Gaussian according to Eq. (57).

Figure 6 shows the conditional PDFs, $P_{x|u}$ and $P_{u|x}$, at $t=1$, 2, and 3. It is seen that LSQKD predicts $P_{x|u}$ and $P_{u|x}$ reasonably well. Moreover, the multimodal shape of $P_{x|u}$ is well predicated by the LSQKD approximation as seen in Figs. 6(a)–6(c). In fact, as time progresses the number of modes increases for $P_{x|u}$. On the other hand, $P_{u|x}$ remains unimodal with increasing time. $P_{u|x}$ obtained by MC is slightly skewed at all times and the conditional PDF deviates from a Gaussian function as observed in Figs. 6(a)–6(f).

B. Three-dimensional state-space example

We now consider application of the LSQKD approach to the three-dimensional state-space equation, Eq. (44), using a bivariate Gaussian kernel density in the u- and T-state space dimensions of the form

$$P(x,u,T;t) = \alpha(x,t) \frac{\exp\left[-\frac{1}{2}\mathbf{y}^T \Lambda^{-1} \mathbf{y}\right]}{2\pi [\det(\Lambda)]^{1/2}}, \tag{71}$$

where

$$\mathbf{y} = \{u - \mu_u(x,t), T - \mu_T(x,t)\}, \tag{72}$$

and Λ is the time-dependent covariance matrix

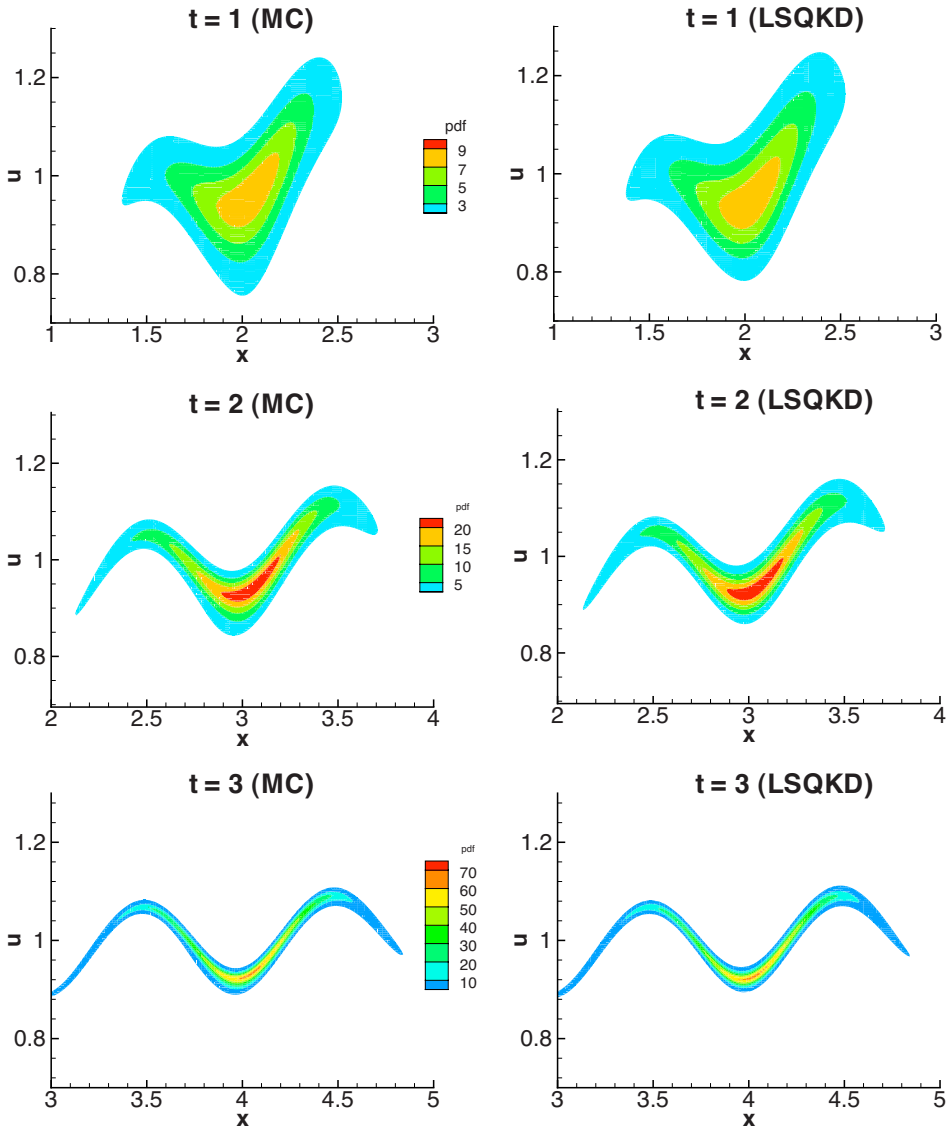

FIG. 5. (Color online) Joint PDF obtained by MC and LSQKD at three times.

$$\Lambda = \begin{pmatrix} \sigma_u^2 & \sigma_u \sigma_T \tanh(\chi) \\ \sigma_u \sigma_T \tanh(\chi) & \sigma_T^2 \end{pmatrix}, \tag{73}$$

with $\sigma_u(x,t), \sigma_T(x,t) > 0$, and $\chi(x,t)$ unconstrained. Use of a hyperbolic tangent mapping for the correlation coefficient was employed for convenience since it ensures the realizability constraint of the u-T covariance at all times. The system of equations derived by the LSQKD method with $\boldsymbol{\xi}_G = \{u, T\}$, reads

$$\frac{\partial \alpha}{\partial t} + \frac{\partial (\mu_u \alpha)}{\partial x} = 0, \tag{74}$$

$$\frac{\partial \mu_u}{\partial t} + \sigma_u^2 \frac{\partial \ln \alpha}{\partial x} + \mu_u \frac{\partial \mu_u}{\partial x} + \frac{\sigma_u}{2} \frac{\partial \sigma_u}{\partial x} - \frac{\sigma_u^2}{2\sigma_T} \frac{\partial \sigma_T}{\partial x} + \frac{\sigma_u^2}{2} \tanh(\chi) \frac{\partial \chi}{\partial x} = \frac{\phi(x,t) - \mu_u}{\tau_p}, \tag{75}$$

$$\frac{\partial \mu_T}{\partial t} + \sigma_u \sigma_T \tanh(\chi) \frac{\partial \ln \alpha}{\partial x} + \mu_u \frac{\partial \mu_T}{\partial x} + \frac{\sigma_u \sigma_T}{2} \frac{\partial \chi}{\partial x} = \frac{\theta(x,t) - \mu_T}{\tau_T}, \tag{76}$$

$$\frac{\partial \sigma_u}{\partial t} + \frac{\partial (\mu_u \sigma_u)}{\partial x} = -\frac{\sigma_u}{\tau_p}, \tag{77}$$

$$\frac{\partial \sigma_T}{\partial t} + \sigma_u \tanh(\chi) \frac{\partial \mu_T}{\partial x} + \mu_u \frac{\partial \sigma_T}{\partial x} = -\frac{\sigma_T}{\tau_T}, \tag{78}$$

$$\frac{\partial \chi}{\partial t} + \frac{\sigma_u}{\sigma_T} \frac{\partial \mu_T}{\partial x} + \mu_u \frac{\partial \chi}{\partial x} = 0. \tag{79}$$

As is apparent by inspecting Eqs. (74)–(79), the main advantage of the LSQKD approximation method is that the three-dimensional Eq. (44) has been transformed into five one-dimensional equations.

The approximation is tested for the case of particles released in a flow with a time-dependent analytical solution of

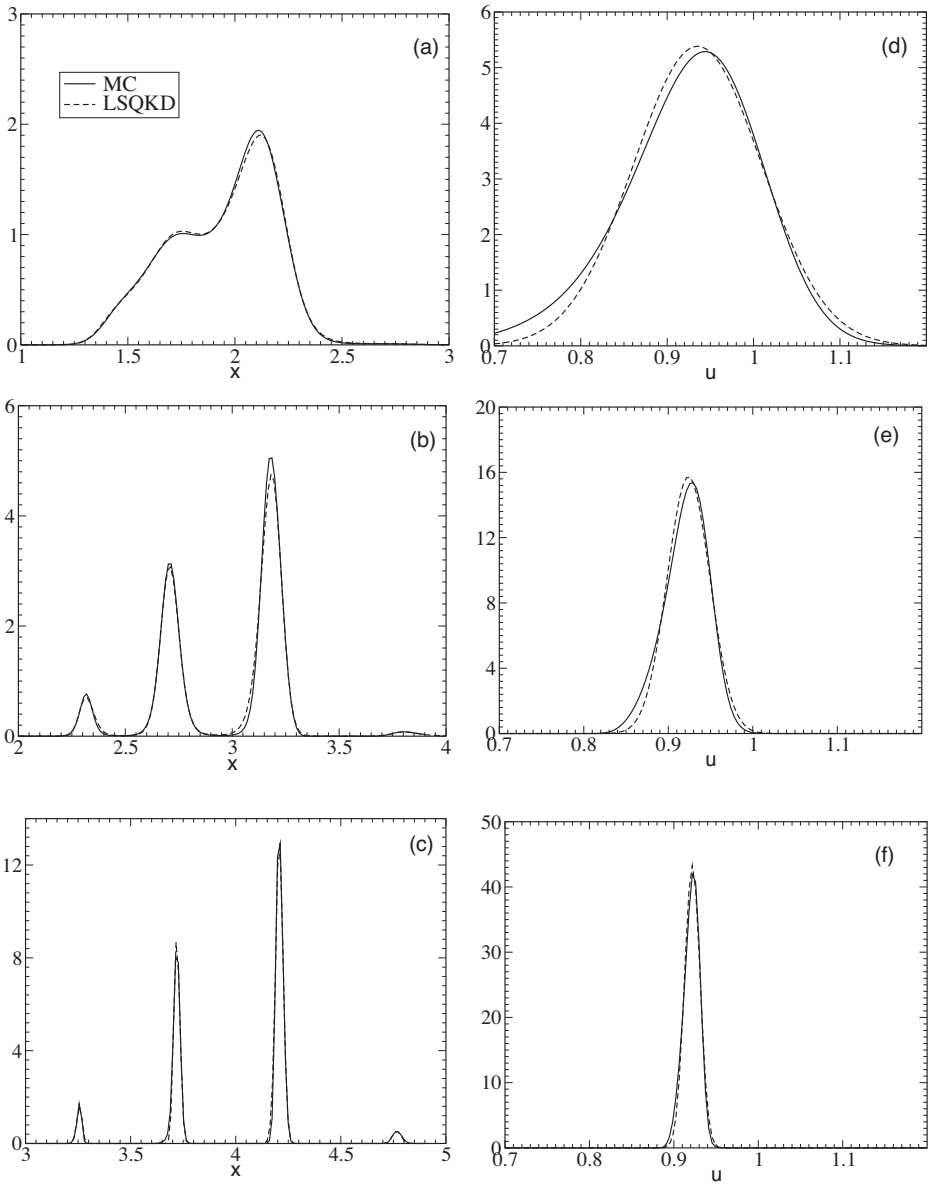

FIG. 6. Conditional PDFs; $P_{x|u}$ at (a) $t=1$, (b) $t=2$, and (c) $t=3$ evaluated at the corresponding $P_{x|u}(x|\langle u_p\rangle(t);t)$ and $P_{u|x}$ at (d) $t=1$, (e) $t=2$, and (f) $t=3$ evaluated at the corresponding $P_{u|x}(u|\langle x_p\rangle(t);t)$.

inviscid flow, given by Riemann (1860) [42]. This corresponds to unidirectional flow in a periodic domain with velocity and temperature solutions given by the implicit relationships

$$\phi(x,t) = v = F\left[x - \left(c_o + \frac{\gamma+1}{2}v\right)t\right] \tag{80}$$

and

$$\theta(x,t) = T = T_o\left(1 + \frac{\gamma-1}{2}v/c_o\right)^2, \tag{81}$$

respectively. The initial condition is chosen to be $F(x,t=0) = u_o \sin(\pi x)$. We integrate Eqs. (74)–(79) using the MC. The parameters used in the evaluation of the method for this three-dimensional state-space problem are chosen as $c_o=1$, $u_o=0.5$, $\tau_p=1$, $\tau_T=0.5$, $\gamma=1.4$, and $T_o=1$. Since this flow develops a shock front at $t=2/[u_o\pi(\gamma+1)]\approx 0.53$, and we have not explored the method in this regime, the time integration was carried out up to $t=0.5$. Figure 7 shows isosurfaces of the final joint PDF when the system is initialized with $\mu_u=0$, $\mu_T=0.5$, $\sigma_u(x,0)=\sqrt{0.05}$, $\sigma_T(x,0)=\sqrt{0.1}$, $\chi(x,0)=0$, and $\alpha(x,0)=G(x,0,\sqrt{0.05})$. Figure 7(a) shows the isosurface $P(x,u,T,0.5)=0.1$ using the MC and Fig. 7(b) shows the same iso-surface using LSQKD; in both cases the surfaces are shown at different angles. We observe that both surfaces are very similar; a result that applies to other isosurface values, not shown. Table I shows comparisons of all means, variances and correlations between MC and LSQKD at $t=0.5$. Reasonable agreement is observed for the low-order moments with relative errors about 0.5% for the means, 0.6% for variances, and up to 1.3% for correlations.

V. DISCUSSION

The computational cost of the approximation method is an important aspect to consider, specially in higher dimensions. We have not investigated exhaustively all computational

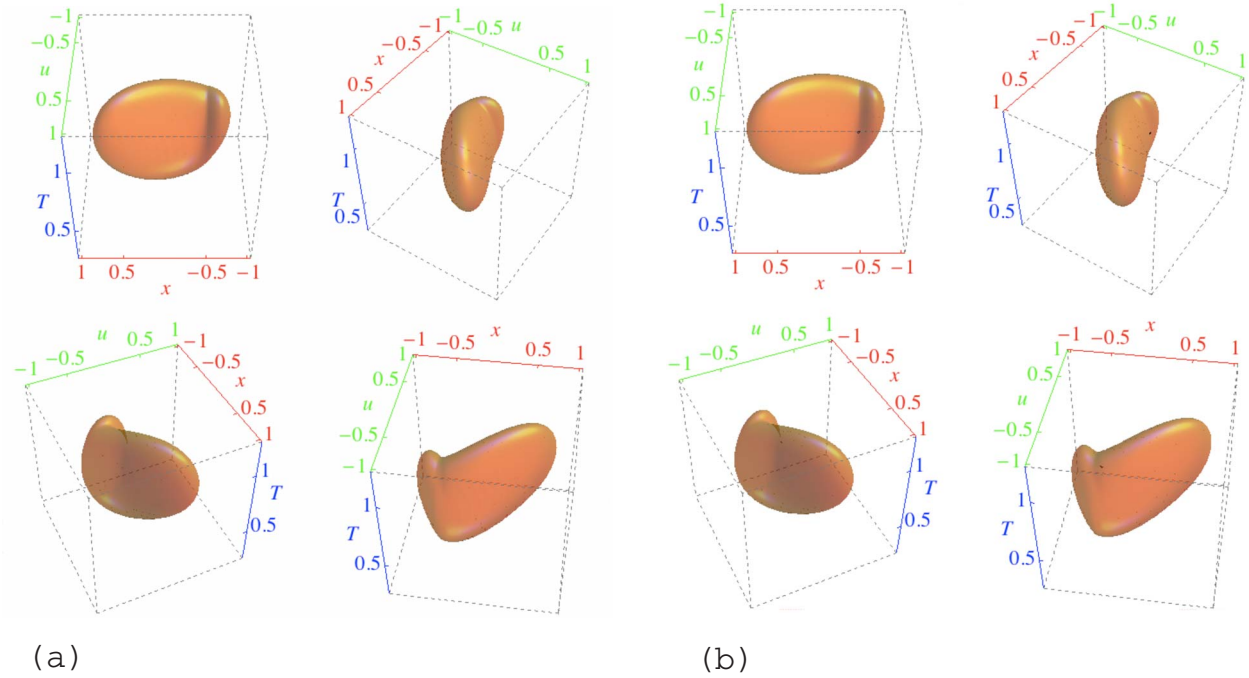

FIG. 7. (Color online) Isosurface of joint position, velocity and temperature PDF, $P(x,u,T;t)=0.1$, at $t=0.5$: (a) From the method of characteristics and (b) from LSQKD. Each subfigure contains four views of the same isosurface at different angles to aid in the understanding of the surface.

considerations of the method in this articlea since we have concentrated on the presentation of the method and its application to a few model problems. From the outset, the savings of the LSQKD are related to the effect of reducing the dimensionality of the method while increasing the number of global parameters. This has to be compared with Liouville's equation, which is a variable coefficient linear equation on the PDF, while the LSQKD method produces quasi-linear systems of equations (coefficients that depend on the dependent variables). In our case, we used a Mathematica™ script to implement all the algorithms and measured 5 s for case 2D using MC and 379 seconds using LSQKD. The results are different for the 3D case, where we measured 5356 seconds using MC and 427 using LSQKD. The discretization of state-space was done consistently by taking the same grid spacing in all cases, with 41^2 and 41^3 grid points for the cases using MC, respectively, and 200 grid points for LSQKD. We observe that solving Eq. (45) by MC is more efficient in two dimensions while a dramatic saving is observed for the three-dimensional case Eq. (44). Evidently solving the quasi-linear equations of LSQKD is not effective in the two-dimensional case but this is quickly overcome in higher dimensions, since the LSQKD cost grows only with the number of parameters and not the dimensionality of the Liouville equation. Note that the time required to obtain the two-dimensional solution up to $t=3$ is similar to that of the three-dimensional problem up to $t=0.5$ simply because solving the velocity and temperature fields, Eqs. (80) and (81), requires substantially more time than Eq. (46).

TABLE I. Comparison of means, variances and correlations using MC and LSQKD at $t=0.5$. Quantities obtained by discretizing the joint PDF on 41^3 grid points centered around the means and extending approximately three standard deviations for both methods.

	MC	LSQKD
$\langle x_p \rangle$	−0.01695	−0.01704
$\langle u_p \rangle$	−0.08664	−0.08704
$\langle T_p \rangle$	0.75977	0.75980
$\langle x_p'^2 \rangle$	0.06891	0.06898
$\langle u_p'^2 \rangle$	0.02757	0.02774
$\langle T_p'^2 \rangle$	0.01569	0.01565
$\langle x_p' u_p' \rangle$	0.03043	0.03066
$\langle x_p' T_p' \rangle$	0.01074	0.01079
$\langle u_p' T_p' \rangle$	0.00456	0.00462
$\langle x_p' u_p' T_p' \rangle$	0.02285	0.02302

A second aspect of the LSQKD method concerns a perceived limitation of the generality of the method; a feature of Rayleigh-Ritz methods. In practice this is not really an obstacle since there is always information about the behavior of the PDF: From the initial and boundary data and by repeatedly solving the equations with increasing resolution; something that is systematically performed with classical methods. In Rayleigh-Ritz methods, increasing the number of trial functions or the number of parameters in the trial functions plays the same role. This approach appears to be less robust, but it is conceptually analogous to increasing resolution. In some cases, it is known that the PDF is unimodal, bimodal or multimodal and this information can help to reduce the cost of solving the multidimensional transport equation for the PDF. Moreover, a global formulation based on a least-squares method already provides a metric of the error. There-

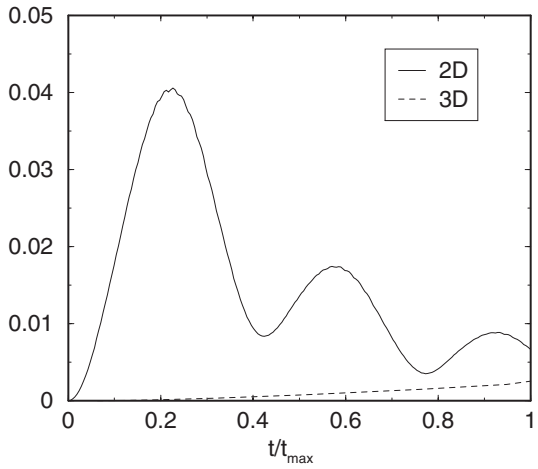

FIG. 8. Normalized residual as a function of time in LSQKD approximation method for 2D and 3D examples.

fore, it can be used to determine whether the trial functions, the KDFs in our case, need to be expanded. This is shown in Fig. 8 for both the 2D and 3D examples. The quantity shown in this figure is the maximum normalized square residual, Eq. (21), over the u and u-T state space as a function of time for the 2D and 3D case, respectively. This is not the error of the PDF but the residual of the transport equation normalized with $\tau_p \sigma_x(0)\sqrt{\sigma_u(0)}$ and $\sqrt{\tau_p \tau_T}\sigma_x(0)\sqrt{\sigma_u(0)\sigma_T(0)}$, respectively. In Sec. IV A 2, the accuracy of the approximation was carefully compared with the MC solution and we observe that the residual of the 3D case is similar to that of the 2D case, therefore justifying the approximations used.

Furthermore, we have verified that the approximation method based on Dirac's delta functions (DQMOM) can be identified with the distinguished limit of LSQKD when using Gaussian KDFs by taking the variance of the Gaussian to the infinitesimally small limit. The Dirac's delta approximation can be recovered in this way without recurring to moment methods explicitly.

Some aspects of the technique presented here that have not been explored include the extension of the present method to bounded state space, instead of the infinite state space considered in this paper. The main difference is that the KDFs must be bounded to the realizability limits of the state space and the quadratures get affected accordingly. The use of more complicated KDFs, for example using three or four parameters, is subject of ongoing research as is the applications where some of the quadratures involved in the least-squares formulation cannot be determined beforehand. In this case, one can use efficient numerical quadratures since the integral kernels are known. The extension to propagation of uncertainty in boundary conditions of systems governed by partial differential equations is also of interest as well as the ability of one function to adapt depending on the behavior of the solution. Finally, another aspect that will be considered in the future is the behavior of the method for very large times, since this is relevant in some problems.

VI. CONCLUSIONS

We present a new approximation technique based on a least-squares method aiming at solving the Liouville equation encountered in the evolution of uncertainty in the initial condition of dynamical systems. The method uses the kernel density function approximation, an ansatz utilized in statistics to approximate the PDF. These presumed shapes are then combined with a least-squares method to determine the evolution equations of the parametrizations of the kernel density functions so that the integrated state-space square error is minimized. In general, the minimization is constrained by the normalization condition of the PDF and requires a Lagrange multiplier approach. This can be handled within the same framework without difficulty. The system of equations resulting from the minimization is linear with respect to the rate of change of the parameters. The coefficients of the system can be nonlinear functions of these parameters. In general, these nonlinear coefficients are obtained from a number of quadratures involving the presumed shaped of the kernel density functions. The main advantage of the method is that, by appropriately choosing the kernel density functions, all the quadratures can be performed explicitly beforehand. Currently, this is carried out with the aid of symbolic manipulation software owing to the complexity of the expressions. It is important to realize that these integrals are performed only once (as part of the setup of the problem) and the only cost of marching the equations in time is associated with solving the system of equations for the rates of change of the parameters. Therefore, the cost of the method is roughly proportional to the number of parameters used to model the PDF and it has the same dimensionality of the original deterministic equations that originate the PDF transport equation. Moreover, since the integrated least-squares residual in state space is known, one can obtain an error metric with little additional cost.

Three problems are considered as models of systems encountered in practice. In the first case we solve the Liouville equation of a system governed by a Riccati equation with initial conditions centered around stable and unstable orbits. The results obtained with the present method for the simplest choice of kernel density function, which is Gaussian, is compared with the analytical solution. It is shown that the results are reasonably good, specially given the crude approximating function used. The second problem involves the Liouville equation in a two- and three-dimensional state space. This problem corresponds to a one-dimensional model of a particle moving in a fluid under the influence of the Stokes force without and with particle internal energy interactions with the flow. In the case that the flow is uniform with constant velocity, a bivariate Gaussian function used in the least-squares approximation is able to predict analytical results while in the case the fluid phase is a nonlinear function, it is not. A better approximation using the least-squares method in the velocity state space gives improved results for this strongly nonlinear forcing case. The improvement is traced to the ability of PDF function to reproduce, or accommodate, the actual joint PDF behavior. The same approach is then used for the particle dynamics including energy exchanges with the fluid with satisfactory results.

ACKNOWLEDGMENTS

The Center for Simulation of Advanced Rockets is sup-

ported by the U.S. Department of Energy through the University of California under Subcontract No. B523819.

[1] M. Ehrendorfer, Meteorologische Zeitschrift **6**, 147 (1977).
[2] M. Ehrendorfer, Mon. Weather Rev. **122**, 703 (1994).
[3] M. Ehrendorfer, Mon. Weather Rev. **122**, 714 (1994).
[4] T. N. Palmer, Rep. Prog. Phys. **63**, 71 (2000).
[5] K. R. James and D. R. Dowling, J. Acoust. Soc. Am. **118**, 2802 (2005).
[6] R. Courant and D. Hilbert, *Methods of Mathematical Physics* (Wiley Interscience, New York, 1989), Vol. 2.
[7] R. Warnock and J. Ellison, *A General Method for Propagation of the Phase Space Distribution, with Application to the Saw-Tooth Instability*, 2nd ICFA Advanced Workshop on Physics of High Brightness Beams, SLAC-PUB-8404, 2000.
[8] A. Lozinski and C. Chauvière, J. Comput. Phys. **189**, 607 (2003).
[9] J. K. Suen, R. Nayak, R. C. Armstrong, and R. A. Brown, J. Non-Newtonian Fluid Mech. **114**, 197 (2003).
[10] C. W. Gardiner, *Handbook of Stochastic Methods* (Springer, Berlin, 1997).
[11] O. P. Le Maître, O. M. Knio, H. N. Najm, and R. G. Ghanem, J. Comput. Phys. **173**, 481 (2001).
[12] D. B. Xiu and G. E. Karniadakis, SIAM J. Sci. Comput. (USA) **24**, 619 (2002).
[13] R. G. Ghanem and P. D. Spanos, *Stochastic Finite Elements, A Spectral Approach* (Dover, New York, 2003).
[14] O. P. Le Maître, H. N. Najm, R. G. Ghanem, and O. M. Knio, J. Comput. Phys. **197**, 502 (2004).
[15] X. Wan and G. E. Karniadakis, SIAM J. Sci. Comput. (USA) **28**, 901 (2006).
[16] R. McGraw, Aerosol Sci. Technol. **27**, 255 (1997).
[17] D. L. Wright, R. McGraw, and D. E. Rosner, J. Colloid Interface Sci. **236**, 242 (2001).
[18] D. L. Marchisio, J. T. Pikturna, R. O. Fox, R. D. Vigil, and A. A. Barresi, AIChE J. **49**, 1266 (2003).
[19] D. L. Marchisio, R. D. Vigil, and R. O. Fox, J. Colloid Interface Sci. **258**, 322 (2003).
[20] R. O. Fox, *Computational Models for Turbulent Reacting Flows* (Cambridge University Press, Cambridge, UK, 2003).
[21] R. Fan, D. L. Marchisio, and R. O. Fox, Powder Technol. **139**, 7 (2004).
[22] D. L. Marchisio and R. O. Fox, J. Aerosol Sci. **36**, 43 (2005).
[23] B. J. Debusschere, H. N. Najm, P. P. Pebay, O. M. Knio, R. G. Ghanem, and O. P. Le Maître, SIAM J. Sci. Comput. (USA) **26**, 698 (2004).
[24] F. Hausdorff, Math. Z. **16**, 220 (1923).
[25] A. Mura and R. Borghi, Combust. Flame **136**, 377 (2004).
[26] A. R. Forsyth, *Calculus of Variations* (Dover, New York, 1960).
[27] S. B. Pope, Flow, Turbul. Combust. **72**, 219 (2004).
[28] P. Lancaster and K. Salkauskas, Math. Comput. **37**, 141 (1981).
[29] K. A. Nguyen, I. Rossi, and D. G. Truhlar, J. Chem. Phys. **103**, 5522 (1995).
[30] T. S. Ho, H. Rabitz, S. E. Choi, and M. I. Lester, J. Chem. Phys. **104**, 1187 (1996).
[31] D. K. Hoffman, G. W. Wei, D. S. Zhang, and D. J. Kouri, Phys. Rev. E **57**, 6152 (1998).
[32] J. Wilkie, M. A. Ratner, and R. B. Gerber, J. Chem. Phys. **110**, 7610 (1999).
[33] G. G. Maisuradze and D. L. Thompson, J. Phys. Chem. A **107**, 7118 (2003).
[34] S. S. Iyengar and M. J. Frisch, J. Chem. Phys. **121**, 5061 (2004).
[35] E. Fix and J. L. Hodges, Technical Report, USAF School of Aviation Medicine, Randolph Field, Texas, 1951 (unpublished).
[36] G. A. Athanassoulis and K. A. Belibassakis, Appl. Ocean. Res. **1**, 1 (2002).
[37] B. W. Silverman, *Density Estimation for Statistics and Data Analysis* (Chapman & Hall, London, 1986).
[38] D. W. Scott, *Multivariate Density Estimation* (Wiley, New York, 1992).
[39] G. A. Athanassoulis and P. N. Gavriliadis, Probab. Eng. Mech. **17**, 273 (2002).
[40] C. L. Lawson and R. J. Hanson, *Solving Least Squares Problems* (Prentice-Hall, Englewood Cliffs, NJ, 1974).
[41] A. Eberle, A. Rizzi, and E. H. Hirschel, *Numerical Solutions of the Euler Equations for Steady Flow Problems* (Vieweg, Braunschweig, 1992).
[42] E. M. Lifshitz and L. D. Landau, *Fluid Mechanics (Course of Theoretical Physics)* (Pergamon Press, New York, 1987).